State-dependent linear-optical qubit amplifier

Karol Bartkiewicz,[1,2,*] Antonín Černoch,[3] and Karel Lemr[1,†]

[1]*RCPTM, Joint Laboratory of Optics of Palacký University and Institute of Physics of Academy of Sciences of the Czech Republic, 17. listopadu 12, 771 46 Olomouc, Czech Republic*

[2]*Faculty of Physics, Adam Mickiewicz University, 61-614 Poznań, Poland*

[3]*Institute of Physics of Academy of Sciences of the Czech Republic, Joint Laboratory of Optics of PU and IP AS CR, 17. listopadu 50A, 772 07 Olomouc, Czech Republic*

(Received 18 September 2013; published 2 December 2013)

We propose a linear-optical setup for heralded qubit amplification with tunable output qubit fidelity. We study its success probability as a function of output qubit fidelity, showing that at the expense of lower fidelity, the setup can considerably increase probability of successful operation. These results are subsequently applied in a proposal for state-dependent qubit amplification. Similar to state-dependent quantum cloning, the *a priori* information about the input state allows us to optimize the qubit amplification procedure to obtain a better fidelity versus success probability trade-off.

DOI: 10.1103/PhysRevA.88.062304 PACS number(s): 03.67.Hk, 42.50.Dv, 03.67.Lx

I. INTRODUCTION

Photons are well suited to be quantum information carriers [1]. Over the past decades, there has been a large number of both theoretically proposed and experimentally tested quantum information protocols designed for photons [2–4]. A notable example with practical applications is quantum cryptography, which allows for unconditionally secure transmission of information [5–9]. One can use both both fiber [10] and free-space [11] optics to distribute photon-encoded information over considerable distances. Even though photons are not so susceptible to interaction with the environment as, for instance, atoms [12], their state also deteriorates because of noise and absorption in the communication channel [13–15].

Since channel transmissivity and level of noise are limited by unavoidable technological imperfections, a viable alternative strategy to increase communication range is based on amplification. However, quantum properties of photon states (unless the state is known *a priori*) are not preserved by classical amplification based on a mere "measure and resend" or stimulated emission approach; thus these approaches are not always suitable [16]. Quantum amplifiers have to be used instead [17–22].

In discrete variable encoding, the polarization or spatial degree of freedom of individual photons is usually used to encode qubits. It is therefore not surprising that optical qubit amplifiers are proposed and built to address these degrees of freedom [23–28]. Similar to other linear-optical quantum gates [29], the qubit amplifiers are also probabilistic, and their successful operation has to be heralded by a specific detection outcome on ancillary photons. Thus apart from amplification gain, one has to introduce success probability to characterize the performance of qubit amplifiers.

In general, a qubit amplifier performs the following transformation on a mixture of vacuum and single-qubit states:

$$p_0|0\rangle\langle 0| + p_1\hat{\rho}_Q \rightarrow \frac{p_0}{N}|0\rangle\langle 0| + \frac{p_1 G}{N}\hat{\rho}'_Q, \qquad (1)$$

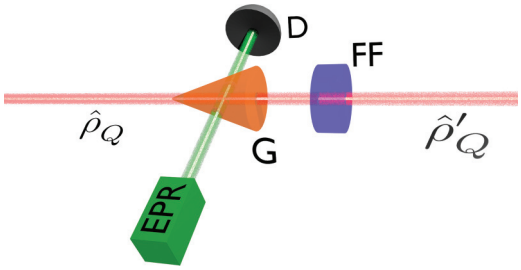

FIG. 1. (Color online) Conceptual scheme of a heralding qubit amplifier. The input state is transformed according to Eq. (1). D, detector; EPR, ancillary photons; G, amplifier: FF, feed forward.

where $\hat{\rho}_Q$ and $\hat{\rho}'_Q$ stand for the input and output qubit density matrices, N denotes normalization, and G is the overall (nominal) gain of the amplifier (see conceptual scheme in Fig. 1). So far, only perfect amplifiers ($\hat{\rho}_Q = \hat{\rho}'_Q$) have been discussed in the literature. In this paper, we extend the analysis of our previously published scheme [28] to the general case of imperfect amplification ($\hat{\rho}_Q \neq \hat{\rho}'_Q$).

This paper is organized as follows: In Sec. II, we describe the principle of operation of the proposed scheme. Moreover we introduce the basic quantities used to characterize our proposed amplifier. We introduce the fidelity of the operation as the overlap between the input and output qubit states. This analysis allows us to establish the success probability versus fidelity trade-off and observe increased success probability at the expense of a fidelity drop that we describe in Sec. III. Finally, in Sec. IV, inspired by optimal state-dependent quantum cloning [30–32], we also show that having some *a priori* information about the input state allows us to optimize the amplification procedure in order to improve this fidelity versus success probability trade-off. We conclude in Sec. V.

II. PRINCIPLE OF OPERATION

In this section we describe the principle of operation of our scheme depicted in Fig. 2 so that in subsequent sections we can analyze the above-mentioned fidelity vs success probability trade-off and state-dependent amplification.

*bartkiewicz@jointlab.upol.cz
†k.lemr@upol.cz

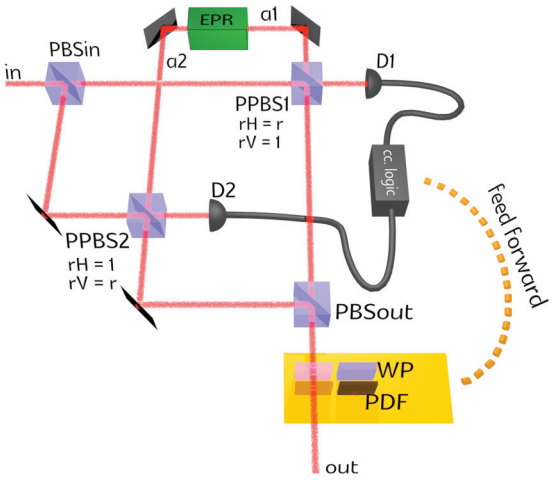

FIG. 2. (Color online) Scheme for a state-dependent linear-optical qubit amplifier as described in the text. EPR, source of entangled ancillary photon pairs; PBS, polarizing beam splitter; PPBS, partially polarizing beam splitter (defined in the text); WP, wave plate; PDF, polarization-dependent filter; D, standard polarization analysis detection block (for reference see [33]).

The signal state $|\psi_s\rangle$ is prepared in superposition of vacuum $|0\rangle$ and polarization-encoded single-qubit state $|Q\rangle$,

$$|\psi_s\rangle = \alpha|0\rangle + \beta|Q\rangle, \tag{2}$$

where $(|\alpha|^2 + |\beta|^2 = 1)$ and the qubit

$$|Q\rangle = \cos\frac{\theta}{2}|H\rangle + \sin\frac{\theta}{2}e^{i\varphi}|V\rangle \tag{3}$$

is parametrized by angles θ and φ describing the superposition of horizontal $|H\rangle$ and vertical $|V\rangle$ polarization basis states. The amplifier also makes use of an ancillary pair of entangled photons in a state parametrized by angle $\chi \in [0; \frac{\pi}{4}]$,

$$|\psi_a\rangle = \cos\chi|HH\rangle + \sin\chi|VV\rangle. \tag{4}$$

In the first step, the signal impinges on the first fully polarizing beam splitter PBSin, where the horizontal and vertical components of the signal qubit are separated into their respective modes. In these modes the interaction with the ancillary pairs of photons takes place: the horizontal component of the signal interacts with the first ancillary photon on a partially polarizing beam splitter PPBS1; similarly, the vertical signal component is combined with the second ancillary photon on the partially polarizing beam splitter PPBS2. The partially polarizing beam splitter PPBS1 fully reflects vertically polarized photons and has reflectivity r for horizontal polarization. On the other hand, PPBS2 reflects all horizontally polarized light and has reflectivity r for vertical polarization. Partially polarizing beam splitter PPBS1 can be described in terms of creation operators

$$\begin{aligned}
\hat{a}^\dagger_{\mathrm{in},H} &\to r\hat{a}^\dagger_{\mathrm{out},H} + \sqrt{1-r^2}\hat{a}^\dagger_{D1,H},\\
\hat{a}^\dagger_{a1,H} &\to -r\hat{a}^\dagger_{D1,H} + \sqrt{1-r^2}\hat{a}^\dagger_{\mathrm{out},H},\\
\hat{a}^\dagger_{a1,V} &\to -\hat{a}^\dagger_{D1,V},
\end{aligned}$$

where labeling of modes corresponds to the scheme in Fig. 2. Analogous transformation describes the action of the PPBS2. Projection on diagonal $|D\rangle = (|H\rangle + |V\rangle)/\sqrt{2}$ and antidiagonal $|A\rangle = (|H\rangle - |V\rangle)/\sqrt{2}$ linear polarization is performed in both detection modes $D1$ and $D2$. The resulting signal state is recovered by combing horizontal and vertical components on the output fully polarizing beam splitter PBSout.

One can trace how the individual components of the three-photon total state (signal and ancillary photons) get transformed by the setup assuming postselection on detection of one photon in each detection mode $D1$ and $D2$:

$$\begin{aligned}
|0_{\mathrm{in}}H_{a1}H_{a2}\rangle &\to r|0_{\mathrm{out}}H_{D1}H_{D2}\rangle,\\
|0_{\mathrm{in}}V_{a1}V_{a2}\rangle &\to r|0_{\mathrm{out}}V_{D1}V_{D2}\rangle,\\
|H_{\mathrm{in}}H_{a1}H_{a2}\rangle &\to (2r^2-1)|H_{\mathrm{out}}H_{D1}H_{D2}\rangle,\\
|H_{\mathrm{in}}V_{a1}V_{a2}\rangle &\to r^2|H_{\mathrm{out}}V_{D1}V_{D2}\rangle,\\
|V_{\mathrm{in}}H_{a1}H_{a2}\rangle &\to r^2|V_{\mathrm{out}}H_{D1}H_{D2}\rangle,\\
|V_{\mathrm{in}}V_{a1}V_{a2}\rangle &\to (2r^2-1)|V_{\mathrm{out}}V_{D1}V_{D2}\rangle.
\end{aligned}$$

After the photons in the detection modes get projected to diagonal $|DD\rangle$ or antidiagonal $|AA\rangle$ linear polarization states (both detected photons share the same polarization), the output signal state can be expressed as

$$\begin{aligned}
|\psi_{\mathrm{out1}}\rangle = {}& \frac{\alpha r}{2}(\cos\chi + \sin\chi)|0\rangle\\
&+\frac{\beta x_+}{2}\cos\frac{\theta}{2}|H\rangle + \frac{\beta y_+}{2}\sin\frac{\theta}{2}e^{i\varphi}|V\rangle,
\end{aligned} \tag{5}$$

where

$$\begin{aligned}
x_\pm &= (2r^2-1)\cos\chi \pm r^2\sin\chi,\\
y_\pm &= (2r^2-1)\sin\chi \pm r^2\cos\chi.
\end{aligned} \tag{6}$$

The output state $|\psi_{\mathrm{out1}}\rangle$ is intentionally kept unnormalized to provide a simple expression for success probability in subsequent calculations. Alternatively, the output signal state (also not normalized) takes the form of

$$\begin{aligned}
|\psi_{\mathrm{out2}}\rangle = {}& \frac{\alpha r}{2}(\cos\chi - \sin\chi)|0\rangle\\
&+\frac{\beta x_-}{2}\cos\frac{\theta}{2}|H\rangle - \frac{\beta y_-}{2}\sin\frac{\theta}{2}e^{i\varphi}|V\rangle
\end{aligned} \tag{7}$$

if $|DA\rangle$ or $|AD\rangle$ coincidence is observed (detected photons have mutually orthogonal polarizations).

A feed-forward operation has to be adopted to correct the qubit part of the state given by Eq. (5) to be identical to the qubit part of Eq. (7). This feed-forward transformation consists of polarization-dependent filtrations τ_H and τ_V when $|DD\rangle$ or $|AA\rangle$ coincidence is detected. These filtrations are functions of the ancilla parameter χ and reflectivity r but are signal state independent:

$$\tau_H = \frac{x_-}{x_+}, \quad \tau_V = \frac{y_-}{y_+}. \tag{8}$$

In the case of $|DA\rangle$ or $|AD\rangle$ coincidence detection, additional phase shift (sign flip) is imposed on vertical polarization ($V \to -V$). This process is not lossy, so we assume it is performed in all the subsequently evaluated scenarios.

A. Success probability

For the subsequent analysis, several quantities are crucial. The first is the overall success probability of the procedure

P_{succ}. It can be expressed using the norm of the output state $|\psi_{\mathrm{out1}}\rangle$ and $|\psi_{\mathrm{out2}}\rangle$. Not implementing the lossy feed-forward, the success probability reads

$$\begin{aligned} P_{\mathrm{succ}} &= 2(|\langle\psi_{\mathrm{out1}}|\psi_{\mathrm{out1}}\rangle| + |\langle\psi_{\mathrm{out2}}|\psi_{\mathrm{out2}}\rangle|) \\ &= |\alpha|^2 r^2 + |\beta|^2 \frac{x_+^2 + x_-^2}{2} \cos^2\frac{\theta}{2} \\ &\quad + |\beta|^2 \frac{y_+^2 + y_-^2}{2} \sin^2\frac{\theta}{2}, \end{aligned} \tag{9}$$

where the factor of 2 describes the two equally probable coincidences leading to $|\psi_{\mathrm{out1}}\rangle$ or $|\psi_{\mathrm{out2}}\rangle$. On the other hand, if the feed-forward is implemented, the output states $|\psi_{\mathrm{out1}}\rangle$ and $|\psi_{\mathrm{out2}}\rangle$ are transformed to the forms

$$\begin{aligned} |\psi_{\mathrm{out1FF}}\rangle &= \frac{\alpha r}{2}(\cos\chi + \sin\chi)|0\rangle \\ &\quad + \frac{\beta x_-}{2}\cos\frac{\theta}{2}|H\rangle + \frac{\beta y_-}{2}\sin\frac{\theta}{2}|V\rangle, \\ |\psi_{\mathrm{out2FF}}\rangle &= \frac{\alpha r}{2}(\cos\chi - \sin\chi)|0\rangle \\ &\quad + \frac{\beta x_-}{2}\cos\frac{\theta}{2}|H\rangle + \frac{\beta y_-}{2}\sin\frac{\theta}{2}|V\rangle, \end{aligned} \tag{10}$$

and the corresponding success probability reads

$$\begin{aligned} P_{\mathrm{succ}} &= 2(|\langle\psi_{\mathrm{out1FF}}|\psi_{\mathrm{out1FF}}\rangle| + |\langle\psi_{\mathrm{out2FF}}|\psi_{\mathrm{out2FF}}\rangle|) \\ &= |\alpha|^2 r^2 + |\beta|^2\left(x_-^2\cos^2\frac{\theta}{2} + y_-^2\sin^2\frac{\theta}{2}\right). \end{aligned} \tag{11}$$

B. Amplification gain

A second very important parameter of the amplifier is the gain G, the ratio between the qubit and vacuum components for the amplified state divided by the analogous ratio for the initial input state, as shown in Eq. (1). In general, the gain can differ for horizontal and vertical polarizations. One can easily define the gain for both polarizations in the case where the feed-forward is implemented:

$$G_{\mathrm{HFF}} = \frac{x_-^2}{r^2}, \quad G_{\mathrm{VFF}} = \frac{y_-^2}{r^2}. \tag{12}$$

If the lossy feed-forward is not implemented, the gain can be calculated as the average gain for output states $|\psi_{\mathrm{out1}}\rangle$ and $|\psi_{\mathrm{out2}}\rangle$,

$$G_H = \frac{x_+^2 + x_-^2}{2r^2}, \quad G_V = \frac{y_+^2 + y_-^2}{2r^2}. \tag{13}$$

The overall gain defined in Eq. (1) is obtained by combining the two gains for horizontal and vertical polarization. In the case of applied feed-forward, the overall gain is given by

$$G_{\mathrm{FF}} = \cos^2\frac{\theta}{2}G_{\mathrm{HFF}} + \sin^2\frac{\theta}{2}G_{\mathrm{VFF}},$$

and in the case without the lossy feed-forward (only the phase flip is performed) it is given similarly by

$$G = \cos^2\frac{\theta}{2}G_H + \sin^2\frac{\theta}{2}G_V.$$

C. Amplification fidelity

The last quantity that has to be calculated in this section is the output qubit fidelity F_Q. This fidelity compares the overlap between the qubit state $|Q\rangle$ at the input with the qubit subspace of the output state $|\psi_{\mathrm{outQ}}\rangle$. If the feed-forward is implemented, the fidelity is simply

$$F_{\mathrm{QFF}} = |\langle\psi_{\mathrm{outQ}}|Q\rangle|^2 = \frac{\left(x_-\cos^2\frac{\theta}{2} + y_-\sin^2\frac{\theta}{2}\right)^2}{x_-^2\cos^2\frac{\theta}{2} + y_-^2\sin^2\frac{\theta}{2}}. \tag{14}$$

If only the feed-forward phase correction and not the full lossy transformation is performed, the fidelity of the output qubit reads

$$\begin{aligned} F_{\mathrm{Q}} &= \langle Q|\hat{\rho}_{\mathrm{outQ}}|Q\rangle \\ &= \frac{\left(x_+\cos^2\frac{\theta}{2} + y_+\sin^2\frac{\theta}{2}\right)^2 + \left(x_-\cos^2\frac{\theta}{2} + y_-\sin^2\frac{\theta}{2}\right)^2}{(x_+^2 + x_-^2)\cos^2\frac{\theta}{2} + (y_+^2 + y_-^2)\sin^2\frac{\theta}{2}}, \end{aligned} \tag{15}$$

where $\hat{\rho}_{\mathrm{outQ}}$ is the normalized density matrix of the single-photon subspace, which is a balanced mixture of $|\psi_{\mathrm{out1}}\rangle\langle\psi_{\mathrm{out1}}|$ and $|\psi_{\mathrm{out2}}\rangle\langle\psi_{\mathrm{out2}}|$, with the $V \to -V$ transformation performed on the latter.

III. SUCCESS-PROBABILITY-FIDELITY TRADE-OFF

In this section we investigate the trade-off between success probability P_{succ} and the output-state fidelity F_{QFF}. For this analysis, we fixed the parameters $\alpha = \beta = \frac{1}{\sqrt{2}}$, and we also took into account the lossy feed-forward.

A. Infinite gain

First, we studied this trade-off on the particular case of infinite gain. The infinite gain is an important setting of qubit amplifiers. To achieve this regime, one simply sets $r = 0$. Thus the previously obtained expressions can be considerably simplified. Coefficients $x_+ = x_- = -\cos\chi$ and $y_+ = y_- = -\sin\chi$ become equal, so there is no need for lossy feed-forward any more ($\tau_H = \tau_V = 1$); only $V \to -V$ is performed. Success probability and qubit fidelity take the forms

$$\begin{aligned} P_{\mathrm{succ}} &= |\beta|^2\left(\cos^2\chi\cos^2\frac{\theta}{2} + \sin^2\chi\sin^2\frac{\theta}{2}\right) \\ &= \frac{|\beta|^2}{2}\left[\cos^2\left(\chi - \frac{\theta}{2}\right) + \cos^2\left(\chi + \frac{\theta}{2}\right)\right] \end{aligned} \tag{16}$$

and

$$F_{\mathrm{QFF}} = \frac{\left(\cos\chi\cos^2\frac{\theta}{2} + \sin\chi\sin^2\frac{\theta}{2}\right)^2}{\cos^2\chi\cos^2\frac{\theta}{2} + \sin^2\chi\sin^2\frac{\theta}{2}}, \tag{17}$$

respectively.

Figure 3 shows the dependence of the success probability on output-state fidelity for four different input states parametrized by $\theta = \{\pi/2, 2\pi/5, \pi/3, \pi/4\}$ and $\varphi = 0$. The calculation reveals that there is no improvement in success probability in the case of a balanced input state ($\theta = \pi/2$), and the success probability remains constant and fidelity independent. In contrast to that, the more the input state is unbalanced, the

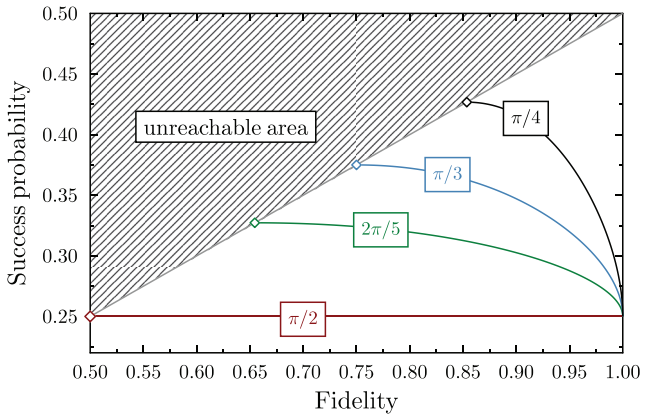

FIG. 3. (Color online) Success probability P_{succ} given by Eq. (16) as a function of output-state fidelity F_{QFF} given by Eq. (17) in the case of infinite gain is depicted for four different input states as described in the text.

more pronounced the dependence of the success probability on fidelity is. This fact will reemerge in Sec. IV, which discusses state-dependent amplification. For instance, in the case of $\theta = \pi/4$, the success probability can be increased by a factor of 1.7 at the expense of 85% output-state fidelity.

B. Maximum success probability

In the next step, we performed a numerical calculation of the maximum achievable success probability for given values of overall gain given by Eq. (1) and the output-state fidelity given by Eq. (14). This calculation has been carried out on the same four input states mentioned above by varying the χ and r parameters. Plots in Fig. 4 present the obtained results,

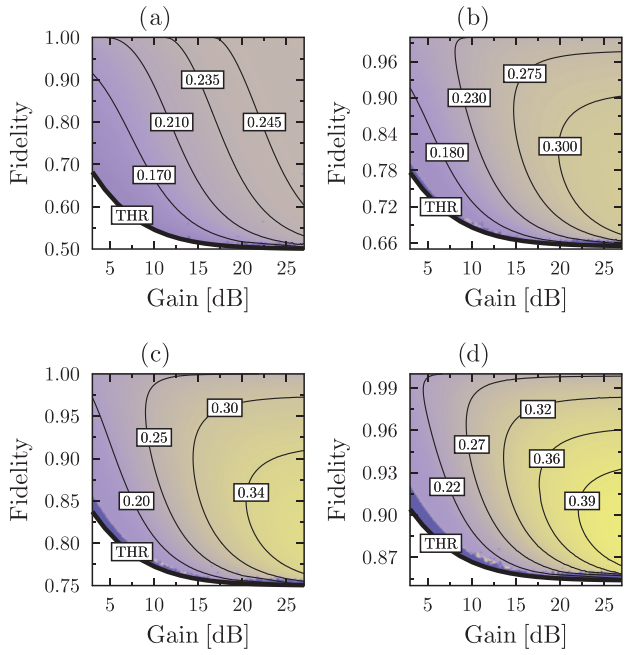

FIG. 4. (Color online) Success probability P_{succ} as a function of both output-state fidelity and amplification gain G_{FF} is depicted for four different input states: (a) $\theta = \pi/2$, (b) $\theta = 2\pi/5$, (c) $\theta = \pi/3$, and (d) $\theta = \pi/4$. THR stands for the threshold of unreachable area.

confirming the finding described in Fig. 3. In addition, one can observe that when set to lower values of gain, the setup performs better for higher fidelities than for lower ones. In the case of higher gains, however, the setup behaves as described in the infinite-gain analysis. Also we were able to establish a state-dependent unreachable area, a set of gain and fidelity coordinates that cannot be reached by the presented setup. This area is visualized by the threshold (TRH) line shown in Fig. 4.

IV. STATE-DEPENDENT AMPLIFICATION

This section brings forward the main result of the paper: how can we improve the success probability of amplification given some *a priori* knowledge about the input qubit state? For the purpose of quantifying the *a priori* information about the input signal, we use the von Mises–Fisher distribution [34] (also known as the Kent distribution) describing dispersion on a sphere. This probability density function is defined as

$$g(\theta,\kappa) = \frac{\kappa}{4\pi \sinh(\kappa)} \exp(\kappa \cos\theta), \tag{18}$$

where θ is the input-state parameter describing the axial angle of the state on the Poincaré sphere and κ, i.e., the concentration parameter, determines the amount of knowledge about the input qubit. Figure 5 depicts the probability distribution over the Poincaré sphere for various values of κ. Note that in the case of $\kappa = 0$, all states are equally probable (therefore no *a priori* knowledge), and the larger the concentration parameter κ is, the more precise the information about the input state is. This trend is illustrated in Table I, which provides the values of medians θ_m and first deciles θ_d for various values of κ. Note that while throughout this paper we center the

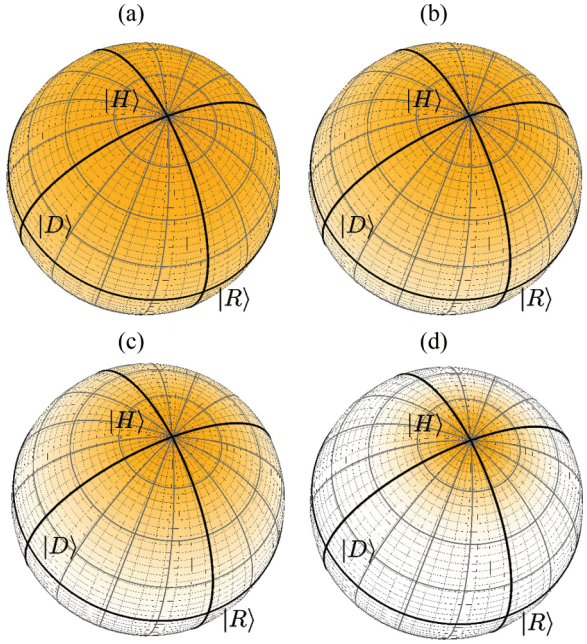

FIG. 5. (Color online) Probability density function $g = g(\theta,\kappa)$ given by Eq. (18) over the Poincaré sphere for various values of the κ parameter used in subsequent numerical simulations: (a) $\kappa = 0$, (b) $\kappa = 1$, (c) $\kappa = 3$, (d) $\kappa = 10$. Labels $|H\rangle$, $|D\rangle$, and $|R\rangle = (|H\rangle + i|V\rangle)/2$ denote the position of the horizontal, diagonal, and right-hand circular-polarization states, respectively.

TABLE I. Values of medians and first deciles of the von Mises–Fisher distribution for several values of the concentration parameter κ.

Parameter κ	Median θ_m (rad)	First decile θ_d (rad)
0	$\pi/2$	0.205π
1	0.357π	0.136π
3	0.220π	0.085π
10	0.119π	0.046π

distribution $g(\kappa,\theta)$ around the northern pole of the sphere (horizontal polarization), the generality of our scheme does not suffer by this choice. If the knowledge about the input state is not centered around the north pole, one can always perform a deterministic rotation to make it so and inverse it after the state comes out of the amplifier. Using this quantification of input-state knowledge, we performed a series of numerical calculations with the goal being to determine the fidelity-success-probability trade-offs. Our results show the relation between the highest achievable average success probability,

$$\langle P_{\mathrm{succ}}\rangle = \int_{\Omega} g(\theta,\kappa) P_{\mathrm{succ}}\, d\omega,$$

for the fixed values of average gain and fidelity,

$$\langle G\rangle = \int_{\Omega} g(\theta,\kappa) G_{\mathrm{FF}}\, d\omega,$$

$$\langle F\rangle = \int_{\Omega} g(\theta,\kappa) F_{\mathrm{QFF}}\, d\omega,$$

respectively, where $d\omega = -d\cos\theta\, d\phi$ and Ω is the surface of the Poincaré sphere. Only the $\langle F\rangle$ integral is not trivial since F_{QFF} is a rational function of $\cos\theta$; thus it was calculated numerically. However, the other integrals can be expressed as linear functions of $\langle\cos\theta\rangle = \coth\kappa - 1/\kappa$. The investigated cases are depicted in Fig. 6. In each case we targeted one specific average overall gain value from the set $\langle G\rangle \in \{3\,\mathrm{dB}, 10\,\mathrm{dB}, 20\,\mathrm{dB}, \infty\}$, where the average was taken over input states distributed according to the von Mises–Fisher distribution for four different values of $\kappa \in \{0; 1; 3; 10\}$. For all the average gain and κ combinations, we determined the relation between the average output-state fidelity and the average success probability. Note that similar to the previous section, we assumed $\alpha = \beta = \frac{1}{\sqrt{2}}$ and we also took into account the lossy feed-forward.

Similar to the case analyzed in Sec. III, not all the values of fidelity are accessible simply because the setup cannot produce fidelity lower than a certain threshold that depends on the values of κ and average gain. It is a very expected result that for the combination of $\kappa = 0$ and infinite gain, the success probability of the setup and fidelity are state independent. This result can be analytically verified using formulas from Sec. II for $r = 0$. In contrast, for other than infinite average gains, there is always a maximum of success probability depending on κ. For $\kappa \to \infty$, this maximum is found for unit fidelity $\langle F\rangle = 1$. It follows from the above-mentioned observations that for a given value of average gain $\langle G\rangle$ and κ, there exists a specific fidelity value $\langle F\rangle$ giving maximum success probability $\max_{\langle F\rangle}\langle P\rangle = P_{\max}$. In some cases this maximum

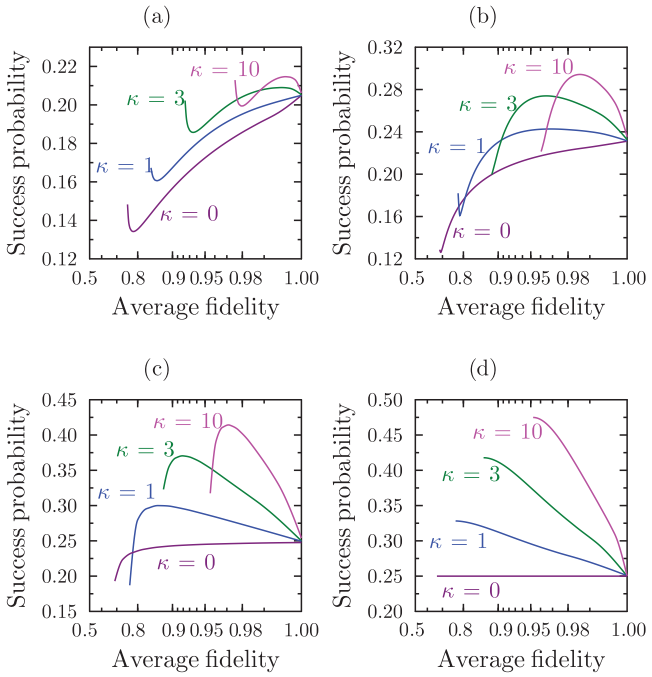

FIG. 6. (Color online) Maximum achievable success probability $\langle P\rangle$ as a function of average fidelity $\langle F\rangle$ for various values of average overall gain [(a) $\langle G\rangle = 3$ dB, (b) $\langle G\rangle = 10$ dB, (c) $\langle G\rangle = 20$ dB, (d) $\langle G\rangle \to \infty$] and state knowledge described by parameter κ of the probability density function $g = g(\theta,\kappa)$ given by Eq. (18).

is to be found on the threshold providing the lower bound on the accessible fidelity values, but surprisingly, this is not always the case. This effect reflects the fact that the space of χ and r values providing, at the same time, the required value of the fidelity and the average gain has a nontrivial structure. Thus it seems that the question about the limits on the success rate of the state-dependent quantum amplifier for fixed amplification parameters does not have a simple answer. Nevertheless, it is apparent that, in general, one can increase the success probability of the setup at the expense of the lower success probability, but sometimes the maximum value $P_{\max}$ can be reached at a lower cost than approaching the fidelity threshold.

A. Merit function

One can argue that some applications require perfect amplification with unit fidelity and thus it is not suitable to increase the success probability of the setup at the expense of lower fidelity. While this may indeed be true in some cases, realistic protocols for quantum communication have to be robust against at least some degree of fidelity drop. This leads us to formulate a figure of merit function inspired by [35]

$$M = \frac{\max\{P_{\mathrm{succ}} F\}}{P_{\mathrm{succ}}(F=1)}, \tag{19}$$

where the numerator is the maximum of the product of fidelity and the corresponding success probability and the denominator is just the success probability at unit fidelity. Since the product of fidelity and success probability can be understood as some sort of output rate of signal qubits, the function M gives the

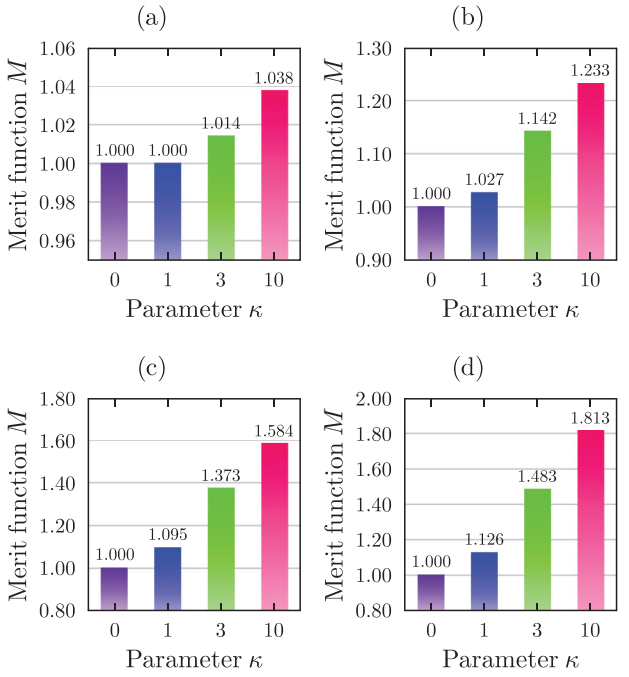

FIG. 7. (Color online) Merit function M given by Eq. (19) depicted for various parameters κ and average gains: (a) $\langle G\rangle = 3$ dB, (b) $\langle G\rangle = 10$ dB, (c) $\langle G\rangle = 20$ dB, (d) $\langle G\rangle \to \infty$.

maximum factor of increased output signal rate if one allows for the fidelity to be smaller than 1 (see Fig. 7).

It can be easily shown that for the very specific case of both infinite average gain and infinite κ, the setup gives exactly the same outcomes of the simple *photon amplifier* [36] based on the "detect and reproduce" method. However, for no *a priori* knowledge about the input state $\kappa = 0$, the setup provides the same functionality as a previously published *qubit amplifier* [28]. In this sense, the setup covers the transition between these two conceptually different devices.

V. CONCLUSIONS

The possibility to operate a qubit amplifier in an imperfect regime, where output qubit fidelity may be smaller than 1, offers a significant increase in success probability if one has some *a priori* information about the input qubit state. In this paper, we analyzed the capabilities of the proposed linear-optical setup for the state-dependent qubit amplifier. We determined the output-state fidelity, gain, and success probability as functions of the setup parameters.

Next, we performed a numerical optimization of success probability depending on target output-state fidelity and gain for various input states. This calculation shows that the closer the state is to the pole of a Poincaré sphere, the more pronounced the success probability improvement is if fidelity is allowed to drop. Also this effect manifests more strongly in the cases of higher gains.

Furthermore we performed numerical analysis of success probability as a function of average output-state fidelity for several target average gains and levels of *a priori* information about the input state quantified by the von Mises–Fisher distribution [34]. The results show how the maximum success probability versus fidelity trade-off behaves depending on average gain and *a priori* information about the input state. To clearly visualize the potential improvement in success probability, we have constructed a specific function of merit that we use to characterize the amplifier in several regimes (various gains and levels of *a priori* knowledge about the input state). This analysis indicate that success probability can be increased on the order of tens of percent depending on the conditions.

Interestingly, we found that, in general (for cases other than infinite gain), the success probability of the amplifier does not increase in a monotonic way for decreasing fidelity. This result clearly demonstrates that the success probability of state-dependent amplifiers can be maximally increased without a significant drop in output-state fidelity. For this reason we believe that our results can stimulate further research on state-dependent qubit amplifiers and their potential applications.

If we draw a comparison between state-dependent amplification and cloning, we will notice a number of similarities. In this paper, we optimize the success probability of the former operation for a given target fidelity, gain, and *a priori* information. In contrast to amplification, cloning schemes are usually optimized to maximize fidelity given certain *a priori* information, disregarding other parameters such as the success probability of the cloning operation. In case of quantum cloning, the analysis of the fidelity vs success probability trade-off has been investigated, for instance, in a recent paper on cloning-based amplification [37]. In the relevant paper, fidelity and probability of success are optimized by switching between optimal probabilistic quantum cloning and deterministic classical cloning based on the measure and reproduce method. Drawing a direct comparison between the setup presented in this paper and the cloning-based amplifier is an intricate problem since they perform qualitatively different operations. The scheme presented in this paper removes the vacuum term from the qubit-vacuum superposition, while the cloning-based amplifier duplicates qubits, making the signal more resistant to attenuation.

The presented analysis assumes the existence of perfect photon-number-resolving detectors and a perfect source of ancillary photons. In an experimental setting, however, one has to take into account the actual properties of laboratory setup components. Experimental imperfections will negatively affect the performance of the setup. For example, if the detectors do not resolve photon numbers, the amplifier will impose a lower gain than predicted. This is because in some cases it is possible for all photons to leak into detection modes, leaving a vacuum at the output; at the same time the operation is misleadingly heralded as successful. Such additional heralding would increase the success probability of the amplification. On the other hand, lower detection efficiency will not affect amplification gain, only lower the success rate. One of the key ingredients in our scheme is a pair of ancillary photons. Their preparation is crucial for this device to function correctly. The fidelity of the amplifier operation depends on how accurately this ancillary photon pair is prepared. Higher photon number contributions generated in the process of spontaneous parametric down-conversion can negatively affect amplification. In such cases the device may yield a "false success" and, instead of amplifying the input

state, send superfluous photons from the ancillary mode to the output port. Failing to deliver ancillary states will result in device malfunction. Therefore ancillary photon-source efficiency imposes a limit on the success rate of the amplifier. The functioning of the proposed setup is affected by a number of other factors, the detailed analysis of which falls beyond the scope of this paper.

ACKNOWLEDGMENTS

The authors gratefully acknowledge the support by the Operational Program Research and Development for Innovations–European Regional Development Fund (Project No. CZ.1.05/2.1.00/03.0058). A.Č. acknowledges Project No. P205/12/0382 of the Czech Science Foundation. K.B. and K.L. acknowledge support from Grant No. DEC-2011/03/B/ST2/01903 of the Polish National Science Centre, and K.B. also acknowledges support from the Operational Program Education for Competitiveness–European Social Fund Project No. CZ.1.07/2.3.00/30.0041. K.L. acknowledges the support from the Czech Science Foundation (Project No. 13-31000P). The authors thank Evan Meyer-Scott, Thomas Jennewein, Norbert Lütkenhaus, Jan Soubusta, and Jára Cimrman for inspiration.

[1] N. Gisin and R. Thew, Nat. Photonics **1**, 165 (2007).
[2] M. Nielsen and I. Chuang, *Quantum Computation and Quantum Information* (Cambridge University Press, Cambridge, 2002).
[3] S. L. Braunstein and P. van Loock, Rev. Mod. Phys. **77**, 513 (2005).
[4] D. Bruß and G. Leuchs, *Lectures on Quantum Information* (Wiley-VCH, Berlin, 2006).
[5] C. H. Bennett and G. Brassard, in *Proceedings of IEEE International Conference on Computers, Systems, and Signal Processing, Bangalore, India, December 10–12, 1984* (IEEE, New York, 1984), pp. 175–179.
[6] C. H. Bennett, F. Bessette, G. Brassard, L. Salvail, and J. Smolin, J. Cryptol. **5**, 3 (1992).
[7] A. K. Ekert, Phys. Rev. Lett. **67**, 661 (1991).
[8] T. C. Ralph, Phys. Rev. A **61**, 010303 (1999).
[9] N. Gisin, G. Ribordy, W. Tittel, and H. Zbinden, Rev. Mod. Phys. **74**, 145 (2002).
[10] S. Wang, W. Chen, J.-F. Guo, Z.-Q. Yin, H.-W. Li, Z. Zhou, G.-C. Guo, and Z.-F. Han, Opt. Lett. **37**, 1008 (2012).
[11] R. Ursin *et al*., Nat. Phys. **3**, 481 (2007).
[12] H. P. Specht, C. Nölleke, A. Reiserer, M. Uphoff, E. Figueroa, S. Ritter, and G. Rempe, Nature (London) **473**, 190 (2011).
[13] Ş. K. Özdemir, K. Bartkiewicz, Y. X. Liu, and A. Miranowicz, Phys. Rev. A **76**, 042325 (2007).
[14] E. Halenková, K. Lemr, A. Černoch, and J. Soubusta, Phys. Rev. A **85**, 063807 (2012).
[15] B. Horst, K. Bartkiewicz, and A. Miranowicz, Phys. Rev. A **87**, 042108 (2013).
[16] M. Oishi, T. Tsuritani, and K. Nishimura, http://dx.doi.org/10.1364/NFOEC.2012.NTu1J.1.
[17] G. Y. Xiang, T. C. Ralph, A. P. Lund, N. Walk, and G. J. Pryde, Nat. Photonics **4**, 316 (2010).
[18] F. Ferreyrol, M. Barbieri, R. Blandino, S. Fossier, R. Tualle-Brouri, and P. Grangier, Phys. Rev. Lett. **104**, 123603 (2010).
[19] A. Zavatta, J. Fiurášek, and M. Bellini, Nat. Photonics **5**, 52 (2010).
[20] C. I. Osorio, N. Bruno, N. Sangouard, H. Zbinden, N. Gisin, and R. T. Thew, Phys. Rev. A **86**, 023815 (2012).
[21] M. Mičuda, I. Straka, M. Miková, M. Dušek, N. J. Cerf, J. Fiurášek, and M. Ježek, Phys. Rev. Lett. **109**, 180503 (2012).
[22] N. A. McMahon, A. P. Lund, and T. C. Ralph, arXiv:1307.7415.
[23] N. Gisin, S. Pironio, and N. Sangouard, Phys. Rev. Lett. **105**, 070501 (2010).
[24] D. Pitkanen, X. Ma, R. Wickert, P. van Loock, and N. Lütkenhaus, Phys. Rev. A **84**, 022325 (2011).
[25] M. Curty and T. Moroder, Phys. Rev. A **84**, 010304(R) (2011).
[26] S. Kocsis, G. Y. Xiang, T. C. Ralph, and G. J. Pryde, Nat. Phys. **9**, 23 (2013).
[27] M. Bula, K. Bartkiewicz, A. Černoch, and K. Lemr, Phys. Rev. A **87**, 033826 (2013).
[28] E. Meyer-Scott, M. Bula, K. Bartkiewicz, A. Černoch, J. Soubusta, T. Jennewein, and K. Lemr, Phys. Rev. A **88**, 012327 (2013).
[29] J. L. O'Brien, Science **318**, 1567 (2007).
[30] G. Chiribella, G. M. D'Ariano, P. Perinotti, and N. J. Cerf, Phys. Rev. A **72**, 042336 (2005).
[31] K. Bartkiewicz and A. Miranowicz, Phys. Rev. A **82**, 042330 (2010); K. Bartkiewicz, A. Miranowicz, and Ş. K. Özdemir, *ibid.* **80**, 032306 (2009).
[32] K. Lemr, K. Bartkiewicz, A. Černoch, J. Soubusta, and A. Miranowicz, Phys. Rev. A **85**, 050307(R) (2012); K. Bartkiewicz, K. Lemr, A. Černoch, J. Soubusta, and A. Miranowicz, Phys. Rev. Lett. **110**, 173601 (2013).
[33] E. Halenková, A. Černoch, K. Lemr, J. Soubusta, and S. Drusová, Appl. Opt. **51**, 474 (2012).
[34] R. A. Fisher, Proc. R. Soc. London, Ser. A **217**, 295 (1953).
[35] K. Lemr, A. Černoch, J. Soubusta, and M. Dušek, Phys. Rev. A **86**, 032321 (2012).
[36] T. C. Ralph and A. P. Lund, in *Proceedings of 9th International Conference on Quantum Measurement and Computing*, edited by A. Lvovsky (AIP, New York, 2009), p. 155.
[37] K. Bartkiewicz, A. Černoch, K. Lemr, J. Soubusta, and M. Stobińska, arXiv:1310.1768.